Journal of Alloys and Compounds 480 (2009) 863–866

Contents lists available at ScienceDirect

Journal of Alloys and Compounds

journal homepage: www.elsevier.com/locate/jallcom

Microstructure, mechanical properties and thermal shock resistance of ZrO_2–$LaPO_4$ composites

Zhongqiu Li*, Jiachen Liu, Shun Li, Haiyan Du

Key Laboratory of Advanced Ceramics and Machining Technology of Ministry of Education, Tianjin University, Tianjin 300072, China

ARTICLE INFO

Article history:
Received 21 December 2008
Received in revised form 11 February 2009
Accepted 14 February 2009
Available online 4 March 2009

Keywords:
Ceramics
Composites
Mechanical properties
Microstructure
Scanning electron microscopy

ABSTRACT

4YSZ–$LaPO_4$ composites with different $LaPO_4$ content ranging from 0 to 30 vol.% were prepared. Influence of $LaPO_4$ content on the microstructure, mechanical properties and thermal shock resistance under mild thermal conditions of the composites were investigated. With the increased content of monazite $LaPO_4$, Vickers hardness, flexural strength and fracture toughness of the 4YSZ–$LaPO_4$ composites exhibited a gradual degradation, while the thermal shock resistance was improved obviously. Results showed that the critical thermal shock temperature (ΔT_c) of 4YSZ/30 vol.% $LaPO_4$ composite under air quenching was 1400 °C, which was 400 °C higher than that of monolithic 4YSZ. Improvement of thermal shock resistance for 4YSZ–$LaPO_4$ composites was mainly due to the higher ratio value of K_{Ic}/σ and the crack deflection and bridging at weak bonding interface between ZrO_2 and $LaPO_4$.

1. Introduction

Dense zirconia ceramics are materials with important technological applications due to their unique combination of excellent properties, such as strength, toughness, chemical stability, refractory characteristics and corrosion resistance [1–3]. However, the poor thermal shock resistance, resulting from the high thermal expansion coefficient and low thermal conductivity, largely limited their actual applications.

Thermal shock resistance is a major issue for ceramics applied under high temperature environment. According to the classic theory on the thermal shock behavior of brittle ceramics established by Hasselman [4,5], increased thermal shock resistance can be achieved either by making it more difficult for cracks to initiate or by limiting the extent to which they can grow once cracking has started. Obtaining useful improvements to the thermal shock resistance by preventing the initiation of cracks is difficult, particularly when the thermal shock is severe, as the crack driving forces can be many orders of magnitude greater than the resistance to fracture of ceramic materials. It is therefore more usual to try to limit the extent of crack propagation. This requires either that as much energy as possible be dissipated in growing the crack, or that the crack driving force available to each individual crack be reduced.

In recent years, some literatures reported that the incorporation of a particulate second phase (e.g., molybdenum [6], Fe_3Al [7], Al_2TiO_5 [8], h-BN [9], AlN [10] and ZrB_2 [11]) into dense zirconia matrix could lead to an enhanced thermal shock resistance. The improvement of thermal shock resistance was largely attributed to the crack shielding and blunting and crack deflection. While the composites have an improved thermal shock resistance, the usefulness of them is limited by their sensitivity to oxidation.

Monazite $LaPO_4$ is a suitable and effective oxide interface material, which exhibits high stability at high temperature in both reducing and oxidizing environment and shows good chemical compatibility with ZrO_2 [12]. The $ZrO_2/LaPO_4$ interface is weak enough to prevent crack growth by interfacial debonding and crack deflection [13]. Therefore, it is expected that the thermal shock resistance can be improved without compromising the excellent refractoriness of zirconia ceramics. In this paper, influence of $LaPO_4$ content on the thermal shock resistance of dense 4YSZ–$LaPO_4$ composites under mild thermal condition was investigated.

2. Experimental procedure

Commercial available Y_2O_3 (99%, Zibo rare earth material Co. Ltd., Shandong, China), ZrO_2 (99.5%, 0.5 μm, Fanmeiya powder Co. Ltd., Jiangxi, China) and $LaPO_4$ (99%, Zibo rare earth material Co. Ltd., Shandong, China) powders were used as the starting materials. The $LaPO_4$ powder was calcined at 1250 °C for 1 h. The mixtures of ZrO_2, Y_2O_3 and $LaPO_4$ were ball milled for 8 h using nylon pots with high purity zirconia balls, Y_2O_3–$LaPO_4$ ranging from 0 to 30 vol.%. The milled slurry was dried at 100 °C in a baking oven and then sieved through an 80 mesh. The dried powder mixture was uniaxially pressed at 200 MPa into rectangular green compacts (30 mm × 7 mm × 4 mm) and then cold isostatic pressed at 250 MPa. The green samples were pressureless-sintered in air at 1550 °C for 2 h according to our existing preparation conditions.

Bulk density of the sintered specimens was measured by the Archimedes displacement method with distilled water, and the theoretical density was estimated

---

* Corresponding author. Tel.: +86 2227891940; fax: +86 2227404724.
E-mail address: midling@yahoo.cn (Z. Li).

0925-8388/$ – see front matter © 2009 Elsevier B.V. All rights reserved.
doi:10.1016/j.jallcom.2009.02.076

Table 1
Calculated m-ZrO_2 content of ZrO_2–$LaPO_4$ composites.

Sample	ZLa0	ZLa10	ZLa15	ZLa20	ZLa30
V_{mt} (vol.%) before thermal shock	1.7	2.3	5.3	5.5	12.5
V_{mt} (vol.%) after thermal shock	2.5	4.1	8.5	12.7	31.1
$\Delta(V_{mt})$	0.7	1.8	3.2	7.2	18.6

by the rule of mixtures. Sintered specimens for flexural strength test were machined into bars with dimensions of 25 mm × 5 mm × 2.5 mm, and the top and bottom surfaces were ground flat and polished by standard diamond polishing techniques down to 1 μm. The edges of all the specimens were chamfered to minimize the effect of stress concentration due to machining flaws. The flexural strength of the specimens was tested using a conventional three point flexural method, with a span of 20 mm and a cross-head speed of 0.368 mm/min. Measurements were performed on at least five test bars of each material.

Hardness (Hv) and fracture toughness (K_{IC}) at room temperature were determined from Vickers indentation tests (HV-10 Vickers hardness tester) on polished surfaces with indentation loads of 98 and 196 N during times of 15 s, respectively. No chipping associated with any indentation was detected, and the indentations that exhibited secondary radial cracking were rejected. The principal diagonals of the plastically deformed zone and the length of the radial cracks were measured using the optical microscopy equipped on HV-10 Vickers hardness tester. The equation proposed by Niihara [14] was used to calculate the K_{IC}. Reported Hv and K_{IC} values are the average of ten determinations and errors are the standard deviations. The young's modulus and thermal expansion coefficient of ZrO_2–$LaPO_4$ composites were calculated by Eq. (1) [15]:

$$E = E_1 V_1 + E_2 V_2 \tag{1}$$

where subscripts 1 and 2 denote ZrO_2 and $LaPO_4$, respectively. V is the volume fraction.

The microstructures of sintered, polished and fractured specimens (after ultrasonic cleaning with acetone and dried) were examined using a Philips XL-30 scanning electron microscope (SEM). XRD analysis was carried out using Rigaku D/max 2500 v/pc X-ray diffractometer (Cu Kα, Ni filter). The volume fraction of the m-ZrO_2 (V_m) was calculated by measuring the intensities of (1 1 1) and (−1 1 1) reflections of the monoclinic phase and the (1 0 1) peak of the tetragonal phase according to the formula of Toraya et al. [16]:

$$V_m = \frac{1.311 X_m}{1 + 0.311 X_m} \tag{2}$$

$$X_m = \frac{I_m(1\ 1\ 1) + I_m(-1\ 1\ 1)}{I_m(1\ 1\ 1) + I_m(-1\ 1\ 1) + I_t(1\ 0\ 1)} \tag{3}$$

where X_m denotes the integrated intensity ratio, I_m and I_t are the peak intensities of the m-ZrO_2 and t-ZrO_2, respectively. The obtained volume fractions of m-ZrO_2 (V_m) were individually normalized to the volume fractions of ZrO_2 (V_{ZrO_2}) present in each composite as follows:

$$V_{mt} = \frac{V_m \times V_{ZrO_2}}{100} \tag{4}$$

Thermal shock tests were performed by measuring the retained flexural strength after quenching into air from desired temperatures. The bars for thermal shock test were heated to desired temperatures for 20 min in a drop-bottom furnace and then air quenched from elevated temperature to room temperature. Thermal quenching was conducted at 623–1423 °C, which corresponded to thermal shock temperature differences (ΔT) of 600–1400 °C. At least five samples were tested for each temperature difference.

3. Results and discussion

3.1. Phase composition and microstructure

X-ray diffraction patterns in the 2θ range from 20° to 34° of polished surfaces of the composites with different $LaPO_4$ content are shown in Fig. 1. Three phases, monoclinic zirconia, tetragonal zirconia and monazite $LaPO_4$ were observed and no new phase could be found in the XRD patterns. This result indicated that $LaPO_4$ did not react with ZrO_2 at 1550 °C. The content of m-ZrO_2 in the composites increased with increasing $LaPO_4$ content (Table 1). It indicated that more spontaneous martensitic transformation occurred with the increased content of $LaPO_4$ in the ZrO_2–$LaPO_4$ composites during cooling from the sintering temperature.

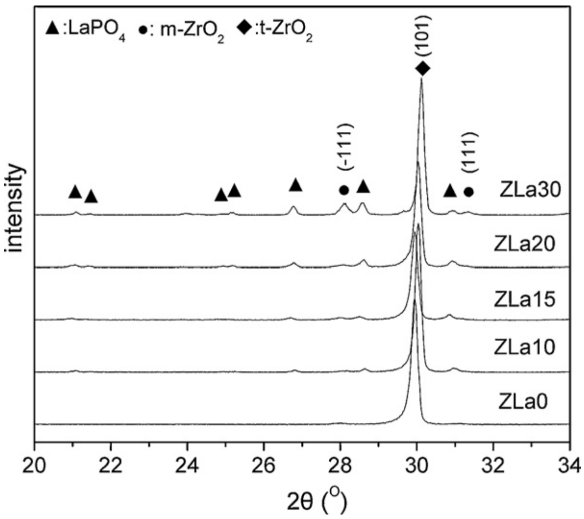

Fig. 1. XRD pattern of ZrO_2–$LaPO_4$ composites with different content of $LaPO_4$.

Fig. 2 is the SEM micrographs of fracture surfaces of monolithic ZrO_2 (ZLa0), ZLa15 and ZLa30. It was observed that ZLa30 had a homogeneous grain size (about 1 μm) distribution. But some abnormal grains over 2 μm could be easily found in the SEM images of ZLa0, ZLa15 ceramics. This indicated that $LaPO_4$ inhibited the abnormal grain growth of ZrO_2 during sintering process. Monolithic ZrO_2 (Fig. 2(a)) shows both intergranular and transgranular fractures, but ZrO_2–$LaPO_4$ composites showed a higher tendency of intergranular fracture, which increased with increasing $LaPO_4$ content.

3.2. Mechanical properties

The relative density and mechanical properties of ZrO_2–$LaPO_4$ composites with different $LaPO_4$ content are shown in Table 2. The relative density of all the sintered composites was above 98%, which was closed to the theoretical density and was consistent with the dense microstructure in Fig. 2.

The hardness, flexural strength and Vickers toughness decreased with increasing $LaPO_4$ content. The decrease of Vickers hardness was directly due to the addition of soft $LaPO_4$ (Young's modulus of $LaPO_4$ is ~100 Gpa). Because of the weak-bonding interfaces between $LaPO_4$ and ZrO_2, when samples were fractured, less energy was required with the increased content of $LaPO_4$, thus resulting in the decrease of flexural strength.

Table 2
Mechanical and thermal properties of ZrO_2–$LaPO_4$ composites.

Material	ZLa0	ZLa10	ZLa15	ZLa20	ZLa30
Relative density (%)	98.9	98.2	98.8	98.7	98.9
σ (MPa)	778 ± 73	681 ± 58	645 ± 62	581 ± 34	508 ± 85
K_{IC} (MPa/m^2)	4.6	4.2 ± 0.1	4.2	4.1 ± 0.1	3.83
Hardness (GPa)	11.4	10.5 ± 0.1	9.7 ± 0.1	9.2 ± 0.1	8.5
E (GPa)	210	199	194	188	177
σ/E	3.7	3.4	3.3	3.1	2.9
K_{Ic}/σ ($\times 10^{-3}$)	5.9	6.2	6.5	7.0	7.5

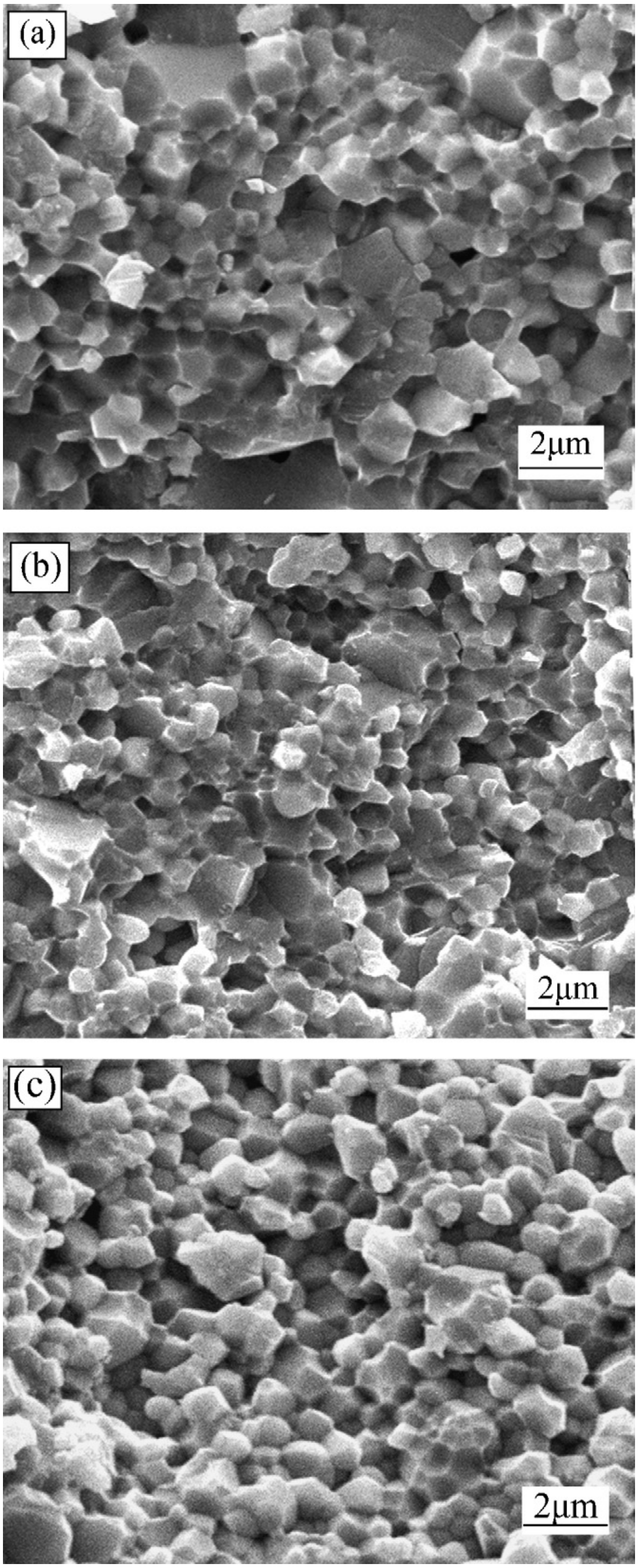

Fig. 2. SEM images of the fracture surfaces of (a) ZLa0 showing both transgranular and intergranular fracture, (b) ZLa15 and (c) ZLa30 showing mainly intergranular fracture, the grain size of ZLa30 is evener than that of ZLa15.

When the composite was fractured, part of t-ZrO_2 would transform to m-ZrO_2, which is known as the stress-induced phase transformation [17]. If more t-ZrO_2 transformed to m-ZrO_2 during the fabrication, the transformation toughening decreased during fracture. It was shown in Table 1 that the content of m-ZrO_2 increased with increasing $LaPO_4$ content. In addition, the Young's modulus and fracture energy decreased with increasing $LaPO_4$ content. Consequently, the toughness of the composites decreased with increasing $LaPO_4$ content.

3.3. *Thermal shock resistance*

In the Hasselman's theory, the residual strength of material after quenching is an important index to estimate the thermal shock resistance. In the current study, specimens of the ZrO_2–$LaPO_4$ composites were subjected to a range of temperature differentials by air quenching. The retained flexural strength was then measured in the same way as in Section 2. The residual strength of ZrO_2–$LaPO_4$ composites as a function of thermal shock temperature is shown in Fig. 3. It was shown that the critical thermal shock temperature (ΔT_c) of ZLa0 and ZLa10 were 1000 °C, indicating that the thermal shock resistance of ZrO_2 was not improved remarkably by adding 10 vol.% $LaPO_4$. The ΔT_c of ZLa15 was 1200 °C, which was almost the same to that of ZLa20. In the experiment, the highest ΔT_c (about 1400 °C) was obtained by ZLa30 composites.

The conditions for crack initiation and propagation in ceramics had been extensively analyzed by Hasselman [2]. The condition for stable and unstable crack growth were predicted based on the idea that the driving force for crack propagation was provided by the stored elastic strain energy. A number of thermal shock parameters (R parameters) were defined to relate thermo-physical and thermo-mechanical properties of the materials to their thermal shock resistance. The effect of microstructure on thermal shock behavior of ZrO_2–$LaPO_4$ composite could be demonstrated by using the parameters:

$$R' = \frac{k\sigma(1-\nu)}{E\alpha} \tag{5}$$

$$R^{\mathrm{IV}} = \frac{K_{\mathrm{Ic}}^2}{\sigma^2(1-\nu)} \tag{6}$$

where k is thermal conductivity, σ is the strength, E is the Young's modulus, α is the thermal expansion coefficient, and ν is the Pois-

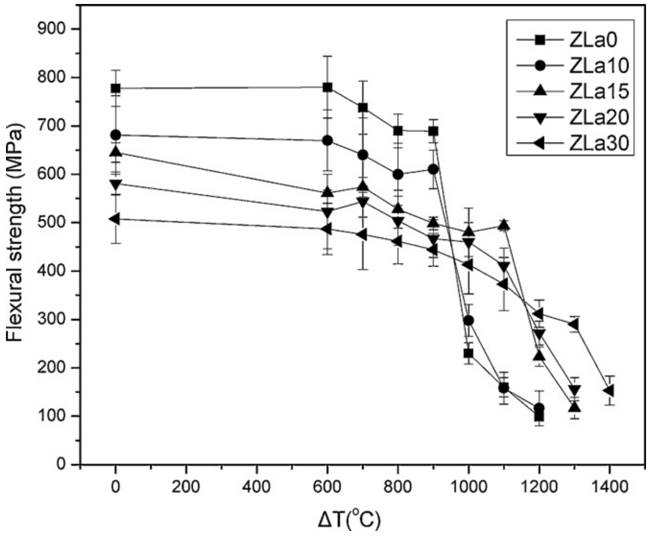

Fig. 3. Plot of temperature differential versus retained strength for ZrO_2–$LaPO_4$ composites.

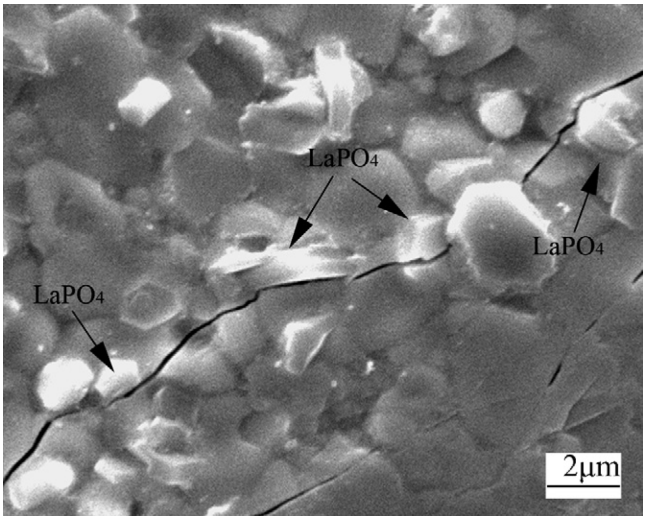

Fig. 4. Thermal shock induced cracking for ZLa15 composite under $\Delta T = 1300\,^\circ$C.

son ratio. The R' parameter provided a measure of the resistance to crack initiation, while the resistance to crack propagation could be gauged from the R^{IV} parameter. Higher value of R' and R^{IV} predicated a higher thermal shock resistance. Because the thermal conductivity and the thermal expansion coefficient of ZrO_2 was very close to those of $LaPO_4$ [18], and the Poisson ratio was almost a fixed value for ZrO_2–$LaPO_4$ composites, the value size of R' and R^{IV} could be determined by σ/E and K_{Ic}/σ, respectively. The calculated value of σ/E and K_{Ic}/σ for ZrO_2–$LaPO_4$ composites were also listed in Table 2. The calculated σ/E value decreased with increasing $LaPO_4$ content, implying that a decreasing critical temperature differential would be expected. This was opposite to the experimental result in Fig. 3. It was possible that micro-cracks in the composites did indeed initiated for a relatively low ΔT, but that the high damage resistance of the composites resulted in minimal crack propagation and consequent strength degradation. Such a claim was also supported by the calculated value of K_{Ic}/σ, which was increased with increasing $LaPO_4$ content.

The results of the SEM and energy spectrum indicated that the weak interfaces between ZrO_2 and $LaPO_4$ particles and the layered structure of $LaPO_4$ played the very important role in resisting the propagation of thermal shock induced micro-cracks. The evidence was shown in Fig. 4. It could be observed that the thermal shock induced crack was discontinuous and propagated along the interfaces between $LaPO_4$ and ZrO_2. The crack deflection and divergence would lead to a partial relief of the thermoelastic strain energy and hence, contributed to resistance to crack propagation. Moreover, the increasing phase transformation of zirconia in ZrO_2–$LaPO_4$ composites would contribute to the resistance to crack propagation (Table 1). Consequently, stable crack propagation was possible during air quenching, thus minimizing the strength degradation as demonstrated in the strength versus air quenching temperature response of the ZrO_2–$LaPO_4$ composite (Fig. 3).

4. Conclusions

4YSZ–$LaPO_4$ composites with different $LaPO_4$ content ranging from 0 to 30 vol.% were prepared. Microstructure, mechanical properties and several parameters relevant to the thermal shock resistance including critical temperature differential, R' and R^{IV} were evaluated and discussed. With the increased content of $LaPO_4$, the Vickers hardness, flexural strength and toughness of the composites decreased gradually, but the thermal shock resistance was improved obviously.

The critical temperature differential of thermal shock resistance for the ZLa30 composite was found to be higher than for monolithic 4YSZ (ZLa0) experimentally as much as 400 °C. Higher ratio value of K_{Ic}/σ and the crack deflection at weak bonding interface between ZrO_2 and $LaPO_4$ were the main factors to improve the thermal shock resistance of the 4YSZ–$LaPO_4$ composites.

Acknowledgements

This research was supported by the National High Technology Research and Development Program of China (863 program) under grant No. 2006AA03Z540, and the National Natural Science Foundation of China under grant No. 50772073.

References

[1] G.W. Liu, W. Li, G.J. Qiao, H.J. Wang, J.F. Yang, T.J. Lu, J. Alloy Compd. 470 (2009) 163–167.
[2] I. Ganesh, J.M.F. Ferreira, Ceram. Int. 35 (2009) 259–264.
[3] Z.G. Liu, J.H. Ouyang, Y. Zhou, J. Li, J. Alloy Compd. 468 (2009) 350–355.
[4] D.P.H. Hasselman, J. Am. Ceram. Soc. 46 (11) (1963) 535–540.
[5] D.P.H. Hasselman, J. Am. Ceram. Soc. 52 (1969) 600–604.
[6] L.D. Schwartz, C.M. Lukaniuk, T.H. Etsell, Adv. Eng. Mater. 1 (1999) 111–113.
[7] J. Li, Y.S. Yin, X.Y. Tan, J.D. Zhang, J. Am. Ceram. Soc. 88 (1) (2005) 235–238.
[8] B. Zhu, S. Ma, J. Bu, Z. Wang, J. Sun, J. Chinese Ceram. Soc. 36 (2) (2008) 228–232.
[9] X. Zhang, R. Zhang, G. Chen, W. Han, Mater. Sci. Eng. A 497 (2008) 195–199.
[10] R.L. Wang, Z.F. Wang, J.L. Bu, L.F. Zhang, Key. Eng. Mater. 368–372 (Pt 1) (2008) 778–780.
[11] X. Zhang, W. Li, C. Hong, W. Han, J. Han, Scripta Mater. 59 (2008) 1214–1217.
[12] P.E.D. Morgan, D.B. Marshall, J. Am. Ceram. Soc. 78 (6) (1995) 1553–1563.
[13] J.B. Davis, D.B. Marshall, R.M. Housley, P.E.D. Morgan, J. Am. Ceram. Soc. 81 (8) (1998) 2169–2175.
[14] K. Niihara, R. Morena, D.P.H. Hasselman, J. Mater. Sci. Lett. 1 (1) (1982) 13–16.
[15] Z.H. Zhou, P.D. Ding, S.H. Tan, J.S. Lan, Mater. Sci. Eng. A 405 (2005) 272–276.
[16] H. Toraya, M. Yoshimura, S. Somiya, J. Am. Ceram. Soc. 67 (1984) 119–121.
[17] R.H.J. Hannink, P.M. Kelly, B.C. Muddle, J. Am. Ceram. Soc. 83 (2000) 461–487.
[18] M. Wu, K. Daimon, T. Matsubara, Y. Hikichi, Mater. Res. Bull. 37 (2002) 1107–1115.